Accepted version of: W. P. du Plessis, P. F. Potgieter, M. Gouws, and E. Malan, “Initial Results for Compressive Sensing in Electronic Support Receiver Systems,” *2011 Saudi International Electronics, Communications and Photonics Conference*, 24-26 April 2011, pp. 1-6. Published version available online:

http://ieeexplore.ieee.org/arnumber=5876908

Initial Results for Compressive Sensing in Electronic Support Receiver Systems

W. P. du Plessis, P. F. Potgieter, M. Gouws, and E. Malan
Defence, Peace, Safety and Security (DPSS)
Council for Scientific and Industrial Research (CSIR)
Pretoria, South Africa, 0001
Email: wduplessis@csir.co.za

***Abstract*—The agile bandwidths of modern radars mean that Electronic Support (ES) receivers require wide instantaneous bandwidths leading to high data rates. Compressive sensing is shown to be a promising technique for reducing data rates for a number of representative radar waveforms. Real-time hardware implementation of compressive sensing is shown to be achievable with modern signal-processing technologies. Compressive sensing thus holds tremendous potential for use in ES systems.**

***Keywords*—Electronic warfare, data compression, compressive sensing.**

I. Introduction

Electronic Support (ES) is that branch of Electronic Warfare (EW) concerned with extracting as much information as possible from an adversary's transmissions (both intentional and unintentional). ES is thus based on receiver technology and considers the interception, detection, characterisation, classification, and identification of emitters. The designation ES is relatively modern and the term Electronic/Electromagnetic Support Measures (ESM) was used historically [1], [2].

Modern ES receiver systems are based on digital receivers allowing powerful signal processing techniques to be used [3], [4]. Recent developments in sampling technology allow wide bandwidths and high dynamic ranges to be achieved, thereby driving performance improvements in ES systems. For example, the CSIR is developing an ES system with a sampling rate of 2 GS/s and a resolution of 10 bits.

However, the rapidly improving performance of digital samplers has meant that the sheer volume of data being generated is becoming impractical. Even the fastest interconnection technologies are pushed to their limits and the largest data storage technologies are filled in periods far too short to be operationally useful.

Compressive sensing is a relatively new technology that has the potential to significantly reduce the data rates associated with ES systems without noticeably affecting their performance [5], [6]. This is achieved by transforming received signals to a domain where less information is required to represent the received signals. This transformation allows the number of data points required to represent a signal or a number of signals to be significantly reduced.

This work was supported by the Armaments Corporation of South Africa (Armscor) under contract KT521896.

Initial results that indicate the potential that compressive sensing shows for application in ES systems are presented. Compressive sensing is shown to allow the possibility of using current data transfer and storage technologies to handle the extremely high data rates of modern digital receivers without compromising performance.

Section II highlights the challenges associated with the extremely high data rates of modern digital receivers. Section III provides a brief introduction to compressive sensing, and Section IV considers the application of compressive sensing to typical radar waveforms. Two hardware implementations of compressive sensing are considered in Section V showing that real-time operation is possible. Finally, a brief conclusion and suggestions for future research are provided in Section VI.

II. Data Rates of Modern ES Systems and Their Effect on System Performance

The extremely high data rates of modern ES systems and their implications for ES system performance are briefly reviewed in this section.

The bandwidth requirement for ES systems is a result of the wide agile bandwidths of modern radar systems. The agile bandwidth of a radar is the range of frequencies over which the radar can operate, and should not be confused with a radar's instantaneous bandwidth which is the bandwidth of the radar's receiver system. The agile bandwidth is largely determined by the antenna and microwave system comprising the transmitter and receiver, while the instantaneous bandwidth is mainly determined by the Analog-to-Digital Converter (ADC) in the receiver. A radar can thus operate at any frequency within its agile bandwidth, but is only able to consider a band equal to the instantaneous bandwidth at any instant.

The International Telecommunication Union (ITU) allocates the band of frequencies from 8.5 to 10.5 GHz to radiolocation (radar) as a primary service in Region 1 [7]. This 2 GHz band represents a bandwidth of only 21%, so it is reasonable to assume that all modern X-Band radars will use at least this range of frequencies as their agile bandwidth.

Modern Digital Radio-Frequency Memory (DRFM) systems are based on 2 GS/s, 10 bit ADCs [8], [9], yet these extremely capable systems only achieve analog bandwidths on the order of 800 MHz due to inevitable filtering requirements to avoid aliasing. This is only 40% of the 2 GHz radar bandwidth at

X Band, so systems with even wider bandwidths are required. With this in mind, the CSIR is conducting initial work towards the development of DRFM systems based on 5 GS/s, 10 bit ADCs to obtain a 2 GHz analog bandwidth. Impressive though these systems are, ADC technology has progressed to the point that 12.5 GS/s, 8 bit ADCs are commercially available [10].

Both DRFM and ES systems consider the same radar systems and thus have comparable bandwidth requirements, however the way bandwidth is viewed differs significantly. DRFM systems should have instantaneous bandwidths wide enough to cover a radar's entire agile bandwidth to ensure that every transmitted pulse is returned. On the other hand, ES systems take a statistical approach to detecting transmissions and are thus not required to intercept every radar pulse. For example, a DRFM system with an 800 MHz instantaneous bandwidth will return only 40% of the pulses from a radar with a 2 GHz bandwidth – an unacceptably low proportion. However, an ES system in the same scenario will have a 40% probability of intercepting any given radar pulse, the ES system will detect one of every ten pulses transmitted by the radar even assuming a detection probability of only 25% – a sufficiently high proportion to be operationally useful.

This suggests that ES systems should be simpler than DRFM systems, but the processing requirements for ES systems are significantly greater. Complex detection and estimation algorithms are required in ES systems (e.g. [3], [4]), while DRFM systems are only required to introduce delays and frequency shifts which may vary over time to modify a simulated target's range and radial velocity (e.g. [1], [2]). ES systems also require multiple channels to perform additional functions such as Angle-of-Arrival (AoA) estimation.

The CSIR and KACST are jointly developing an ES system based on 2 GS/s, 10 bit ADCs. As highlighted above, this system is expected to intercept 40% of the pulses from a radar with a 2 GHz agile bandwidth. However, this result assumes that the data generated by the ADCs can be processed at the same rate as it is generated without any dead time.

The first problem is getting the data transferred from the ADC to an appropriate processor. Serial RapidIO is a widely-used high-speed interface standard [11] that is representative of other data transfer standards. The lastest incarnations of Serial RapidIO (version 2 and later) support up to 6.25 Gbaud per lane and up to 16 parallel lanes [12]. While this would appear to be more than sufficient to handle the 20 Gb/s data rate required, this is not always the case.

Serial RapidIO uses 8b/10b encoding which reduces the line speed of a 6.25 Gbaud lane to a transfer rate of only 5 Gb/s, and protocol overhead will lead to further reductions to 4 Gb/s or less. Even a four-lane, 6.25 Gbaud Serial RapidIO link is thus unable to transfer the 20 Gb/s of data generated by a single ADC. That said, a sixteen-lane, 6.25 Gbaud Serial RapidIO link has a bandwidth on the order of 60 to 64 Gb/s which is sufficient to transfer the data from even a 5 GS/s, 10 bit ADC in the next generation of DRFM and ES systems.

However, implementation of the full sixteen-lane, 6.25 Gbaud Serial RapidIO capability is still relatively rare. For example, Texas Instruments' new TMS320C66x range of multicore Digital Signal Processors (DSPs), announced as recently as 9 November 2010 [13], only has a four-lane, 5 Gbaud Serial RapidIO interface [14]. Texas Instruments' previous TMS320C647x range of DSPs only has a two-lane, 3.125 GBaud Serial RapidIO interface [15], [16].

To make matters worse, the discussion so far has only considered a single ADC channel while ES systems require multiple channels. It thus appears safe to state that modern ES systems generate data at a rate that is too high to be transferred to modern processing systems. Given this reality, the best approach appears to be to buffer the data at the rate at which it is generated and then to transfer the data to processing hardware at a lower data rate. However, this has a negative effect on the probability of intercepting a transmission.

For example, a four-channel, 2 GS/s, 10 bit ES system will generate data at a rate of 80 Gb/s which is 25% more than the optimistic assumption of 64 Gb/s for the fastest Serial RapidIO line. This means that data will take 25% longer to read from memory than it took to write into memory, so the above example will only be sampling 44.4% of the time. Assuming an 800 MHz analog bandwidth, this means that the probability of intercepting a radar pulse in the ITU-allocated radar X-Band is reduced to 17.8%, and the fact that not every pulse can be detected will further reduce this value.

While a 17.8% intercept probability is likely to be acceptable, it should be recalled that these values are based on the maximum bandwidth achievable by the latest version of the Serial RapidIO protocol, and as highlighted above, implementation of this maximum case is by no means universal. For example, the data generated by a four-channel, 2 GS/s, 10 bit ES system will lead to a intercept probability of less than 6% if the Serial RapidIO interface of Texas Instruments' new TMS320C66x range of DSPs is used.

It is thus clear that some means of dramatically reducing the data rates generated by modern ES systems is required.

III. Compressive Sensing

Compressive sensing is a relatively new concept that is able to use data rates significantly lower than the Nyquist rate while still allowing accurate reconstruction of the original signals [5], [6], [17], [18]. Compressive sensing is based on the representation of signals using basis functions, and exploits incoherence and sparsity to reduce the number of symbols required to represent a signal.

The well-known ES process of reducing a signal to its underlying characteristics including frequency, pulse width, and Pulse Repetition Frequency or Interval (PRF or PRI) is similar to the concept of compressive sensing. In both cases, the original, Nyquist-sampled signal is analysed and only that information required to reconstruct the signal is retained. The main difference is that the typical ES parameters listed above are only valid for a very specific class of signals whereas compressive sensing is valid for any compressible signals.

Representing a signal as an N-element column vector $\mathbf{x}$

allows the signal to be written as

$$\mathbf{x} = \mathbf{\Psi c} \tag{1}$$

where $\mathbf{\Psi}$ is an $N \times N$ orthonormal matrix, and $\mathbf{c}$ is an N-element column vector of the coefficients of the signal in the domain defined by $\mathbf{\Psi}$. Examples of bases include the Fourier, discrete cosine, wavelet and Gabor bases (e.g. [19]–[22]).

The first step to applying compressive sensing is finding a domain where the representation is sparse. Sparsity implies that the number of coefficients with significant magnitude in the coefficient vector $\mathbf{c}$ for a given transform $\mathbf{\Psi}$ is much smaller than the number of elements in the original representation $\mathbf{x}$. A signal with S significant coefficients is said to be S-sparse. This requirement makes the reconstruction of the original signal possible and will be considered further below.

Compressive sensing works by applying a transformation to the original samples of a signal

$$\mathbf{y} = \mathbf{\Phi x} \tag{2}$$

where $\mathbf{y}$ is the M element compressed version of the signal $\mathbf{x}$ associated with the $M \times N$ measurement ensemble $\mathbf{\Phi}$. The ratio M/N is known as the compression ratio and indicates the data reduction that is achieved. Expanding the signal using (1) allows (2) to be rewritten as

$$\mathbf{y} = \mathbf{\Phi\Psi c} \tag{3}$$

$$= \mathbf{\Theta c} \tag{4}$$

where $\mathbf{\Theta}$ is a constant $M \times N$ matrix known as the holographic basis [17]. The role of the holographic basis is to project an N-dimensional space onto a M-dimensional space – the foundation of compressive sensing.

The form of (3) and (4) means that only M samples are available in $\mathbf{y}$ to reconstruct $N \gg M$ samples in $\mathbf{c}$, so compressive sensing considers an under-determined system. If $\mathbf{\Phi}$ and $\mathbf{\Psi}$ are coherent or even nearly coherent, $\mathbf{y}$ will only contain information about a small proportion of the samples in $\mathbf{c}$. In the extreme case of perfect coherence, the elements of $\mathbf{y}$ become identical to some elements of $\mathbf{c}$ and reconstruction of the remainder of the elements in $\mathbf{c}$ becomes impossible. The measurement ensemble $\mathbf{\Phi}$ and transformation matrix $\mathbf{\Psi}$ must thus be incoherent for signal reconstruction to be possible. Mathematically, mutual coherence is given by [5], [23]

$$\mu\left(\mathbf{\Phi}, \mathbf{\Psi}\right) = \sqrt{N} \times \max_{1 \le k \le M, 1 \le j \le N} \left|\langle \phi_k, \psi_j \rangle\right| \tag{5}$$

where $\langle \phi_k, \psi_j \rangle$ denotes the inner product of the k^{th} row of $\mathbf{\Phi}$ and the j^{th} column of $\mathbf{\Psi}$. Equation (5) effectively states that mutual coherence is the largest inner product of any measurement ensemble of $\mathbf{\Phi}$ and any basis of $\mathbf{\Psi}$. Lower values of μ indicate lower coherence, indicating that $\mathbf{\Phi}$ and $\mathbf{\Psi}$ are suitable for compressive sensing. When $\mathbf{\Phi}$ and $\mathbf{\Psi}$ are both orthonormal bases, the mutual coherence is limited to values in the range $1 \le \mu \le \sqrt{N}$. (This range is not valid for compressive sensing because the requirement that both $\mathbf{\Phi}$ and $\mathbf{\Psi}$ be orthonormal bases would mean that both must be $N \times N$ matrices.)

TABLE I
MAXIMAL-LENGTH SEQUENCE BANDWIDTHS AND PULSE LENGTHS USED IN SIMULATIONS.

Bandwidth (MHz)	Pulse length (μs)	Sequence length
10	12.60	$2^6 - 1 = 63$
100	10.22	$2^9 - 1 = 511$
500	8.19	$2^{11} - 1 = 2047$

Basis pursuit reconstruction of a signal starts from (4) and solves the convex problem [5], [24]

$$\min_{\hat{\mathbf{c}} \in \Re^N} \|\hat{\mathbf{c}}\|_{\ell_1} \quad \text{subject to} \quad \mathbf{y} = \mathbf{\Theta}\hat{\mathbf{c}} \tag{6}$$

where $\|\hat{\mathbf{c}}\|_{\ell_p} = \sum_i |\hat{c}_i|^p$ is the ℓ_p norm. The fact that $\hat{\mathbf{c}}$ is sparse is a prerequisite for signal reconstruction in (6) because minimisation of the ℓ_1 norm in (6) is only possible when the number of nonzero elements in $\hat{\mathbf{c}}$ is less than or equal to the number of elements in $\mathbf{y}$. Equation (6) can be solved using the well-known interior-point methods (e.g. [25]). However, (6) is not the only way to perform signal reconstruction and that other options exist, notably matching pursuit [26].

The development now naturally moves to consider whether suitable measurement ensembles can be found. The most general requirement for reconstruction to be possible is that the Restricted Isometry Property (RIP) hold for the holographic basis (or equivalently, that a Uniform Uncertainty Principle (UUP) is obeyed). Mathematically, the RIP requires [5]

$$(1 - \delta) \|\mathbf{c}\|_{\ell_2}^2 \le \|\mathbf{\Theta c}\|_{\ell_2}^2 \le (1 + \delta) \|\mathbf{c}\|_{\ell_2}^2 \tag{7}$$

to be valid for all S-sparse vectors $\mathbf{c}$ when $\delta < 1$. Equation (7) implies that a solution will always exist because the energy in the compressed signal is related to the energy in the original signal. When

$$M \ge CS \log\left(N\right) \tag{8}$$

where C is a small constant, the RIP has been shown to hold for a large variety of matrices. Equation (8) effectively states that reconstruction is only possible if the number of elements in $\mathbf{y}$ is sufficiently larger than the number of nonzero elements in $\hat{\mathbf{c}}$ to allow (6) to be solved. An example of a matrix for which the RIP holds is the Bernoulli ensemble where each element is set to to $\pm 1/\sqrt{M}$ with equal probability.

IV. COMPRESSIVE SENSING OF TYPICAL RADAR WAVEFORMS

The application of compressive sensing to ES will be investigated using the following waveforms:

Unmodulated pulse: This signal is typical of older radars.

Linear frequency chirp: Used in many pulse compression and Low Probability of Intercept (LPI) radars.

Binary phase coding: Phase coding is also used in pulse compression, and Maximal-Length (ML) sequences are used here as representative examples.

The signals are filtered with a 100-element FIR filter to ensure that they satisfy the specified bandwidths.

The bandwidths for the frequency chirp and phase-coded signals were varied from 10 MHz to 500 MHz in the steps

TABLE II
RMS ERROR FOR AN UNMODULATED SINUSOID.

Number of samples	Compression ratio				
	0.5	***0.4***	***0.3***	***0.2***	***0.1***
100	0.0724	0.0913	0.1113	0.1354	0.3486
200	0.0507	0.0589	0.0737	0.1257	0.3030
500	0.0290	0.0343	0.0450	0.0663	0.1345
1000	0.0208	0.0273	0.0362	0.0440	0.0778
2000	0.0143	0.0190	0.0255	0.0342	0.0620

shown in Table I. The pulse lengths were set equal to 10 μs for the unmodulated and swept-frequency cases. However, the phase-coded case is limited by the relatively small number of ML sequences and the pulse lengths listed in Table I were thus used to ensure that the bandwidth is correct.

The ES system used in the analysis is based on a 2 GS/s, 10 bit ADC. A baseband centre frequency of 500 MHz was used in all cases to place the signal at the centre of the ADC's band to prevent aliasing at wide bandwidths. The signals are normalized to half the full-scale range of the ADC and a Signal-to-Noise Ratio (SNR) of 10 dB was used.

A Discrete Cosine Transform (DCT) was used as the basis $\mathbf{\Psi}$ because the signals considered are sparse in that domain unless their bandwidths are extremely wide.

A 10 μs pulse will have 20,000 samples when sampled at 2 GS/s, but the number of samples processed simultaneously will be significantly lower than this value. This potential difficulty was overcome by processing N samples at a time after padding the pulse with zeros to ensure that the total number of samples is a multiple of N.

The reconstruction error will be expressed as a Root Mean-Square (RMS) error computed from

$$\mathrm{E} = \sqrt{\frac{1}{P}\sum_{p=1}^{P}(x_p - x_{rp})^2} \tag{9}$$

where x_p and x_{rp} are the P elements of the original and reconstructed signals respectively normalized so that the peak-to-peak amplitude of the original signal is equal to 1.

The results of reconstructing an unmodulated sinusoid are given in Table II. The RMS error is good when both the number of samples and the compression ratio are high but becomes poor when this is not the case. This is perhaps surprising given that an unmodulated sinusoid is extremely sparse in the DCT domain. However, the reconstruction process is unable to uniquely identify the small number of significant coefficients when the number of available samples is small. The situation might be improved by using an alternative transform $\mathbf{\Psi}$ or another reconstruction technique.

The RMS errors obtained when reconstructing the 10 MHz frequency chirp and phase modulated signals are summarized in Tables III and IV. The results are seen to be extremely good unless both the number of samples and the compression ratio are small. The results are better than for the unmodulated sinusoid because the number of significant coefficients is larger. In addition, the RMS error is lower for the frequency chirp than for the phase-modulated signal, suggesting that the chirp is more compressible.

TABLE III
RMS ERROR FOR A 10 MHZ LINEAR FREQUENCY CHIRP.

Number of samples	Compression ratio				
	0.5	***0.4***	***0.3***	***0.2***	***0.1***
100	0.0675	0.0999	0.1260	0.1311	0.2774
200	0.0530	0.0668	0.0841	0.1291	0.2090
500	0.0309	0.0380	0.0522	0.0684	0.1247
1000	0.0207	0.0263	0.0338	0.0457	0.0775
2000	0.0156	0.0188	0.0256	0.0344	0.0572

TABLE IV
RMS ERROR FOR A 10 MHZ PHASE-CODED PULSE.

Number of samples	Compression ratio				
	0.5	***0.4***	***0.3***	***0.2***	***0.1***
100	0.0715	0.0920	0.1150	0.1434	0.3309
200	0.0504	0.0623	0.0795	0.1221	0.3071
500	0.0300	0.0381	0.0519	0.0754	0.1550
1000	0.0220	0.0280	0.0384	0.0510	0.1052
2000	0.0158	0.0196	0.0268	0.0383	0.0812

The 100 MHz frequency chirp and phase modulated signal reconstructions are considered in Tables V and VI. As before, the RMS errors are low in the majority of cases and the chirp signal has lower reconstruction errors than the phase-modulated signal. The main difference is that the error for the phase-modulated signal increases rapidly when compression ratios of 0.2 or less are encountered. This behaviour is anticipated in light of the threshold implied by (8).

Reconstruction of signals with a 500 MHz bandwidth is evaluated in Tables VII and VIII for the frequency chirp and phase-modulated cases respectively. The phase-modulated case follows a similar trend to the previous cases except that the errors are significantly higher due to the larger number of significant coefficients in the DCT domain.

However, the RMS error for the 500 MHz frequency chip first decreases as the number of compressed samples increases as before, but the reaches a minimum and increases thereafter. This rather surprising characteristic is a result of the unique nature of a frequency chirp and can be explained by considering Figure 1. As the number of points N increases, the number of significant coefficients increases because the signal sweeps across a wider band in the time associated with N thereby reducing the signal's sparsity.

The results in Tables II to VIII show that increasing the number of processed and compressed samples (N and M respectively) decreases the RMS error. However, multiplying an $M \times N$ matrix by an N-element column vector in (2) requires MN multiplications and $M\,(N-1)$ additions. The required number of Multiply-Accumulate Cycles per Second (MACS) is given by

$$\mathrm{MACS} = \frac{f_s}{N}MN \tag{10}$$

$$= f_s M \tag{11}$$

where f_s is the sampling rate because the data are considered in blocks of N samples and each compression computation requires MN multiplications. Table IX gives the computational requirements for the measurement ensembles used in

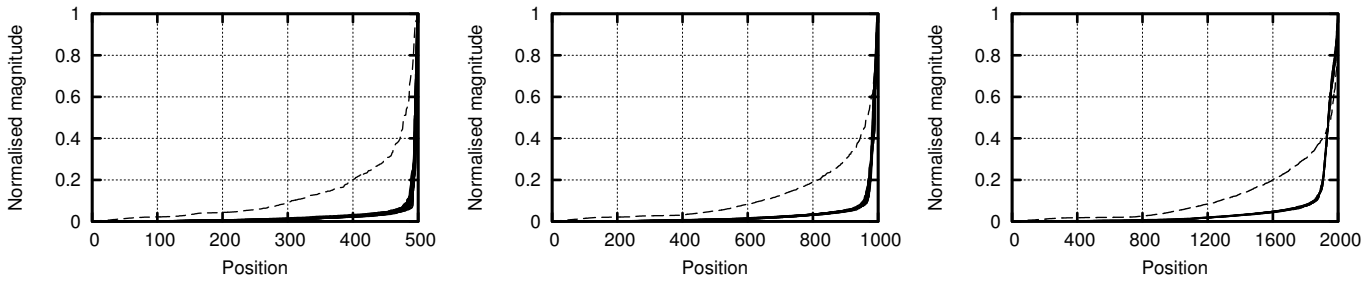

(a) N = 500. (b) N = 1000. (c) N = 2000.

Fig. 1. The normalized DCT coefficient magnitudes of a linear frequency chirp with a 500 MHz bandwidth sorted from smallest to largest for different values of N. The number of coefficients with significant magnitudes increases with N. The dotted lines are the last group of points padded with zeros to have N points.

TABLE V
RMS ERROR FOR A 100 MHZ LINEAR FREQUENCY CHIRP.

Number of samples	Compression ratio				
	0.5	*0.4*	*0.3*	*0.2*	*0.1*
100	0.0764	0.1062	0.1228	0.1684	0.2974
200	0.0552	0.0694	0.0897	0.1339	0.2269
500	0.0343	0.0442	0.0602	0.0753	0.1378
1000	0.0257	0.0335	0.0464	0.0684	0.1215
2000	0.0174	0.0245	0.0375	0.0542	0.1089

TABLE VI
RMS ERROR FOR A 100 MHZ PHASE-CODED PULSE.

Number of samples	Compression ratio				
	0.5	*0.4*	*0.3*	*0.2*	*0.1*
100	0.0745	0.1092	0.1546	0.2538	0.3317
200	0.0528	0.0773	0.1191	0.2104	0.3270
500	0.0364	0.0532	0.0926	0.1766	0.3116
1000	0.0250	0.0364	0.0737	0.1674	0.3010
2000	0.0175	0.0282	0.0600	0.1626	0.2879

TABLE VII
RMS ERROR FOR A 500 MHZ LINEAR FREQUENCY CHIRP.

Number of samples	Compression ratio				
	0.5	*0.4*	*0.3*	*0.2*	*0.1*
100	0.1097	0.1325	0.1590	0.2052	0.3144
200	0.0904	0.1100	0.1346	0.1683	0.2549
500	0.0799	0.0948	0.1121	0.1420	0.2195
1000	0.0771	0.0923	0.1107	0.1525	0.2778
2000	0.0762	0.0988	0.1293	0.2140	0.3416

TABLE VIII
RMS ERROR FOR A 500 MHZ PHASE-CODED PULSE.

Number of samples	Compression ratio				
	0.5	*0.4*	*0.3*	*0.2*	*0.1*
100	0.2180	0.2710	0.3117	0.3467	0.3707
200	0.2124	0.2549	0.2994	0.3484	0.3723
500	0.2101	0.2572	0.3017	0.3414	0.3763
1000	0.2000	0.2519	0.2984	0.3360	0.3733
2000	0.2017	0.2452	0.2924	0.3334	0.3598

Tables II to VIII. There is thus a compromise between the desire to more accurately reconstruct signals by using larger compression ratios and numbers of samples, and the need to perform the necessary computations.

The results considered above only use Bernoulli measurement ensembles and basis pursuit reconstruction. As outlined in Section III, other options are available for both the measurement ensemble and reconstruction, so it is possible that better results could be achieved. Despite this observation, the results presented here demonstrate that successful reconstruction of typical radar waveforms is possible. The natural next question is whether compressive sensing implementations can be fast enough to be useful.

V. HARDWARE IMPLEMENTATIONS AND THEIR IMPLICATIONS FOR ES SYSTEMS

A Bernoulli measurement ensemble was implemented on both a Field Programmable Gate Array (FPGA) and a DSP to evaluate the practical implications of implementing compressive sensing.

A Xilinx Virtex-5 SX95T FPGA in the -2 speed grade [27] was used to implement a Bernoulli ensemble with $M = 32$ and $N = 160$ for a compression ratio of 0.2 which was simulated using Xilinx's System Generator 10.1.1 software. The size of the measurement ensemble was determined by the requirement to compress data from a 2 GS/s, 10 bit ADC data in real time – that is the processing happens at least as fast as the data is generated. Each of the 640 Xilinx "DSP48E Slices" in the Virtex-5 SX95T is capable of performing 500 million multiply-accumulate operations per second, giving a theoretical processing capability of 320 GMACs.

For the DSP implementation, a Bernoulli ensemble with $M = 400$ and $N = 1152$ for a compression ratio of 0.35 was implemented on a Texas Instruments TMS3206474 DSP running at 1.0 GHz. The measurement ensemble size was limited by the requirement that it be hosted in L2 cache to avoid performance penalties due to cache misses. The necessary computations take 578 μs, so this is far too slow to compress data from a 2 GS/s, 10 bit ADC in real time. However, only one of the three available processing cores was used, four compression calculations are preformed simultaneously and the clock speed can be increased to 1.2 GHz, so an improvement of over fourteen times is possible. Furthermore, the new TMS320C6678 has a theoretical processing capability of 320 GMACS for integer computations versus only 23 GMACS for the TMS3206474 running at 1 GHz.

TABLE IX
COMPUTATIONAL COST IN GMACS OF APPLYING COMPRESSIVE SENSING TO THE DATA GENERATED BY A 2 GS/S ADC.

Number of samples	Compression ratio				
	0.5	*0.4*	*0.3*	*0.2*	*0.1*
100	**100**	**80**	**60**	**40**	**20**
200	200	**160**	**120**	**80**	**40**
500	500	400	300	200	**100**
1000	1000	800	600	400	200
2000	2000	1600	1200	800	400

In both the FPGA and DSP cases, the bold computational load values in Table IX should be achievable assuming that 50% of the theoretical maximum processing capability of 320 GMACS is achieved. Real-time compression of data using compressive sensing approaches is thus achievable with modern high-speed FPGAs and DSP processors.

VI. CONCLUSION

This paper started by highlighting the extremely high data rates generated by modern ES systems. These data rates arise naturally from the agile bandwidths of modern radars, so a reduction in sampling rates will lead to unacceptable system performance degradation. Even an operation as simple as merely transferring data from one system to another was shown to be extremely challenging even with the fastest available systems. The need to reduce data rates without compromising the instantaneous bandwidth or dynamic range of ES receivers is thus apparent.

Compressive sensing was introduced as an option to reduce data rates while still allowing accurate reconstruction of the original signals. Compressive sensing was then simulated on representative radar waveforms, and the results are encouraging. Narrowband signals are shown to be accurately reconstructed with reasonable measurement ensemble sizes, though ultra-wideband signals remain a challenge.

Real-time hardware implementation of data compression using compressive sensing approaches was considered and shown to be achievable with modern FPGA and DSP systems.

The successful implementation of compressive sensing in ES systems has thus been shown to be both necessary given radar agile bandwidths and possible in light of existing signal-processing technology.

However, this work only presents initial results and the computationally efficient reconstruction of signals has not been addressed. The significance of this limitation is somewhat diminished by the fact that reconstruction does not need to take place in real time and can be accomplished far from the ES system generating the data. These observations mean that high-performance computing technology can be leveraged for reconstruction. Furthermore, the fact that the power in the compressed signal is related to the power in the original signal by the RIP (7) opens the possibility of performing detection on compressed signals without requiring signal reconstruction (e.g. [28], [29]).

REFERENCES

[1] F. Neri, *Introduction to electronic defense systems*. Artech House, 1991.

[2] D. C. Schleher, *Electronic warfare in the information age*. Artech House, 1999.

[3] J. B.-Y. Tsui, *Digtal techniques for wideband receivers*. Norwood, MA: Artech House, 1995.

[4] P. E. Pace, *Detecting and classifying low probability of intercept radar*. Norwood, MA: Artech House, 2009.

[5] E. J. Candès and M. B. Wakin, "An introduction to compressive sampling," *Signal Processing Magazine, IEEE*, vol. 25, no. 2, pp. 21–30, March 2008.

[6] J. K. Romberg, "Imaging via compressive sampling," *Signal Processing Magazine, IEEE*, vol. 25, no. 2, pp. 14–20, March 2008.

[7] Independent Communications Authority of South Africa, "National frequency plan," South African Government Gazette, 30 July 2010.

[8] (2010, 28 January) Digital RF memories. Micro Systems, Inc. [Online]. Available: http://www.herley.com/pdfs/her7145_DRFM_DS_D1.pdf

[9] (2010, 28 January) New wideband digital RF memory. Kor Electronics. [Online]. Available: http://www.korelectronics.com/component/docman/doc_view/32-10-bit-1-ghz-laboratory-drfm?tmpl=component&format=raw

[10] (2010, 28 January) Data converter modules. Tektronix Component Solutions. [Online]. Available: http://component-solutions.tek.com/about/news-publications/publications/MaxtekDataConverterModules.pdf

[11] (2011, 28 January) Rapidio: Home. RapidIO Trade Association. [Online]. Available: http://www.rapidio.org/home

[12] *RapidIO Interconnect Specification*, RapidIO Trade Association Std., Rev. 2.1, August 2009.

[13] (2010, 9 November) Delivering more than 5x the performance of any DSP in the market, Texas Instruments' new TMS320C66x multicore DSPs set a new standard in innovation and performance. Texas instruments Incorporated. [Online]. Available: http://newscenter.ti.com/Blogs/newsroom/archive/2010/11/09/delivering-more-than-5x-the-performance-of-any-dsp-in-the-market-texas-instruments-new-tms320c66x-multicore-dsps-set-a-new-standard-in-innovation-and-performance-545167.aspx

[14] (2010) TMS320C66x DSP generation of devices. Texas Instruments Incorporated. SPRT580. [Online]. Available: http://www.ti.com/litv/pdf/sprt580

[15] *TMS320C6472 Fixed-Point Digital Signal Processor*, Texas Instruments Incorporated, October 2010, SPRS612E.

[16] *TMS320C6474 Multicore Digital Signal Processor*, Texas Instruments Incorporated, November 2010, SPRS552G.

[17] D. L. Donoho, "Compressed sensing," *IEEE Transactions on Information Theory*, vol. 52, no. 4, pp. 1289–1306, April 2006.

[18] E. J. Candès, J. K. Romberg, and T. Tao, "Robust uncertainty principles: exact signal reconstruction from highly incomplete frequency information," *Information Theory, IEEE Transactions on*, vol. 52, no. 2, pp. 489–509, February 2006.

[19] G. E. Carlson, *Signal and linear system analysis*, 2nd ed. John Wiley, 1998.

[20] V. Britanak, P. C. Yip, and K. R. Rao, *Discrete cosine and sine transforms: General properties, fast algorithms and integer approximations*. Academic Press, 2006.

[21] A. Graps, "An introduction to wavelets," *IEEE Computational Science Engineering*, vol. 2, no. 2, pp. 50–61, 1995.

[22] H. G. Feichtinger and T. Strohmer, *Gabor analysis and algorithms: theory and applications*. Birkhäuser, 1998.

[23] D. L. Donoho and X. Huo, "Uncertainty principles and ideal atomic decomposition," *IEEE Transactions on information Theory*, vol. 47, no. 7, pp. 2845–2862, November 2001.

[24] S. S. Chen, D. L. Donoho, and M. A. Saunders, "Atomic decomposition by basis pursuit," *SIAM Review*, vol. 43, no. 1, pp. 129–159, 2001.

[25] J. Nocedal and S. J. Wright, *Numerical optimization*. Springer, 1999.

[26] S. Mallat and Z. Zhang, "Matching pursuits with time-frequency dictionaries," *IEEE Transactions on Signal Processing*, vol. 41, no. 12, pp. 3397–3415, December 1993.

[27] (2011, 13 February) Virtex-5 SXT FPGAs. Xilinx. [Online]. Available: http://www.xilinx.com/products/virtex5/sxt.htm

[28] M. F. Duarte, M. A. Davenport, M. B. Wakin, and R. G. Baraniuk, "Sparse signal detection from incoherent projections," in *Acoustics, Speech and Signal Processing, 2006. ICASSP 2006 Proceedings. 2006 IEEE International Conference on*, vol. 3, May 2006.

[29] M. A. Davenport, P. T. Boufounos, M. B. Wakin, and R. G. Baraniuk, "Signal processing with compressive measurements," *Journal of Selected Topics in Signal Processing*, vol. 4, no. 2, pp. 445–460, April 2010.